Transmit Energy Focusing for DOA Estimation in MIMO Radar with Colocated Antennas

Aboulnasr Hassanien, *Member, IEEE* and Sergiy A. Vorobyov *Senior Member, IEEE*

Abstract

In this paper, we propose a transmit beamspace energy focusing technique for multiple-input multiple-output (MIMO) radar with application to direction finding for multiple targets. The general angular directions of the targets are assumed to be located within a certain spatial sector. We focus the energy of multiple (two or more) transmitted orthogonal waveforms within that spatial sector using transmit beamformers which are designed to improve the signal-to-noise ratio (SNR) gain at each receive antenna. The subspace decomposition-based techniques such as MUSIC can then be used for direction finding for multiple targets. Moreover, the transmit beamformers can be designed so that matched-filtering the received data to the waveforms yields multiple (two or more) data sets with rotational invariance property that allows applying search-free direction finding techniques such as ESPRIT for two data sets or parallel factor analysis (PARAFAC) for more than two data sets. Unlike previously reported MIMO radar ESPRIT/PARAFAC-based direction finding techniques, our method achieves the rotational invariance property in a different manner combined also with the transmit energy focusing. As a result, it achieves better estimation performance at lower computational cost. Particularly, the proposed technique leads to lower Cramer-Rao bound than the existing techniques due to the transmit energy focusing capability. Simulation results also show the superiority of the proposed technique over the existing techniques.

Index Terms

Direction-of-arrival estimation, MIMO radar, rotational invariance, search-free methods, transmit beamspace.

The authors are with the Department of Electrical and Computer Engineering, University of Alberta, 9107-116 St., Edmonton, Alberta, T6G 2V4 Canada. Emails: {`hassanie, vorobyov `}`@ece.ualberta.ca`

Corresponding author: Sergiy A. Vorobyov, Dept. Elect. and Comp. Eng., University of Alberta, 9107-116 St., Edmonton, Alberta, T6G 2V4, Canada; Phone: +1 780 492 9702, Fax: +1 780 492 1811. Email: `vorobyov@ece.ualberta.ca`.

I. INTRODUCTION

The development of multiple-input multiple-output (MIMO) radar is recently the focus of intensive research [1]-[3]. A MIMO radar is generally defined as a radar system with multiple transmit linearly independent waveforms and it enables joint processing of data received by multiple receive antennas. MIMO radar can be either equipped with widely separated antennas [2] or colocated antennas [3].

Estimating direction-of-arrivals (DOAs) of multiple targets from measurements corrupted by noise at the receiving array of antennas is one of the most important radar applications frequently encountered in practice. Many DOA estimation methods have been developed for traditional single-input multiple-output (SIMO) radar [4]-[12]. Among these methods the estimation of signal parameters via rotational invariance techniques (ESPRIT) and multiple signal classification (MUSIC) are the most popular due to their simplicity and high-resolution capabilities [6], [9], [12]. Moreover, ESPRIT is a special and computationally efficient case of a more general decomposition technique of high-dimensional (higher than 2) data arrays known as parallel factor analysis (PARAFAC) [13], [14].

More recently, some algorithms have been developed for DOA estimation of multiple targets in the context of MIMO radar systems equipped with M colocated transmit antennas and N receive antennas [15]–[19]. The algorithms proposed in [15] and [16] require an exhaustive search over the unknown parameters and, therefore, mandate prohibitive computational cost if the search is performed over a fine grid. On the other hand, the search-free ESPRIT-based algorithms of [17] and [18] as well as PARAFAC-based algorithm of [19] utilize the rotational invariance property of the so-called extended virtual array to estimate the DOAs at a moderate computational cost. It is worth noting that in the case of MIMO radar, the advantages of the aforementioned DOA estimation methods over similar MUSIC- and ESPRIT/PARAFAC-based DOA estimation methods for SIMO radar appear due to the fact that the extended virtual array of MN virtual antennas can be obtained in the MIMO radar case by matched-filtering the data received by the N-antenna receive array to M transmitted waveforms. Therefore, the effective aperture of the virtual array can be significantly extended that leads to improved angular resolution. In the methods of [17]–[19], the rotational invariance property is achieved by partitioning the receiving array to two (in ESPRIT case) or multiple (in PARAFAC case) overlapped subarrays. Then, the rotational invariance is also presumed for the virtual enlarged array of MN virtual antennas. However, the methods of [17]–[19] employ full waveform diversity, i.e., the number of

transmitted waveforms equals the number of transmit antennas, at the price of reduced transmit energy per waveform. In other words, for fixed total transmit energy, denoted hereafter as E, each waveform has energy E/M transmitted omni-directionally. It results in a reduced signal-to-noise ratio (SNR) per virtual antenna. On the other hand, it is well-known that the estimation accuracy of subspace-based techniques suffers from high SNR threshold, that is, the root-mean-squared error (RMSE) of DOA estimates approaches the corresponding Cramer-Rao bound (CRB) only for relatively high SNRs [20], [21]. Therefore, the higher the SNR, the better the DOA estimation performance can be achieved.

It has been shown in [22], [23] that a tradeoff between the SNR gain and aperture of the MIMO radar virtual array can be achieved by transmitting less than M orthogonal waveforms. Exploiting this tradeoff, we develop in this paper[1] a group of DOA estimation methods, which allow to increase the SNR per virtual antenna by (i) transmitting less waveforms of higher energy and/or (ii) focusing transmitted energy within spatial sectors where the targets are likely to be located. At the same time, reducing the number of transmitted waveform reduces the aperture of the virtual array, while a larger aperture may be useful for increasing the angular resolution at high SNR region.

The contributions of this work are based on the observation that by using less waveforms the energy available for each transmitted waveform can be increased, that is, the SNR per each virtual antenna can be improved, while the aperture of the virtual array decreases to KN, where $K \leq M$ is the number of orthogonal waveforms. Moreover, the SNR per virtual antenna can be further increased by focusing the transmitted energy in a certain sector where the targets are located. Our particular contributions are as follows. The transmit beamformers are designed so that the transmitted energy can be focussed in a certain special sector where the targets are likely to be located that helps to improve the SNR gain at each receive antenna, and therefore, improve the angular resolution of DOA estimation techniques, such as, for example, MUSIC-based techniques. Moreover, we consider the possibility of obtaining the rotational invariance property while transmitting $1 < K \leq M$ orthogonal waveforms using different transmit beamforming weight vectors and focusing the transmitted energy on a certain spatial sector where the targets are located. It enables us to design search-free ESPRIT/PARAFAC-based DOA estimation techniques. In addition, we derive CRB for the considered DOA estimation

---

[1]An early exposition of a part of this work has been presented in [24].

schemes that aims at further demonstrating how the DOA estimation performance depends on the number of transmitted waveforms, transmit energy focusing, and effective array aperture of the MIMO radar virtual array.

The paper is organized as follows. In Section II, MIMO radar signal model is briefly introduced. In Section III, we present the transmit beamspace-based MIMO radar signal model. Two approaches for designing the transmit beamspace weight matrix are given in Section IV. In Section V, we present MUSIC and ESPRIT DOA estimation for transmit beamspace-based MIMO radar. Performance analysis and CRB are given in Section VI. Simulation results which show the advantages of the proposed transmit beamspace-based MIMO radar DOA estimation techniques are reported in Section VII followed by conclusions drawn in Section VIII.

II. MIMO Radar Signal Model

Consider a MIMO radar system equipped with a transmit array of M colocated antennas and a receive array of N colocated antennas. Both the transmit and receive antennas are assumed to be omni-directional. The M transmit antennas are used to transmit M orthogonal waveforms. The complex envelope of the signal transmitted by the mth transmit antenna is modeled as

$$s_m(t) = \sqrt{\frac{E}{M}} \phi_m(t), \quad m = 1, \ldots, M \tag{1}$$

where t is the fast time index, i.e., the time index within one radar pulse, E is the total transmitted energy within one radar pulse, and $\phi_m(t)$ is the mth baseband waveform. Assume that the waveforms emitted by different transmit antennas are orthogonal. Also, the waveforms are normalized to have unit-energy, i.e., $\int_T |\phi_m(t)|^2 dt = 1$, $m = 1, \ldots, M$, where T is the pulse width.

Assuming that L targets are present, the $N \times 1$ received complex vector of the receive array observations can be written as

$$\mathbf{x}(t, \tau) = \sum_{l=1}^{L} r_l(t, \tau) \mathbf{b}(\theta_l) + \mathbf{z}(t, \tau) \tag{2}$$

where τ is the slow time index, i.e., the pulse number, $\mathbf{b}(\theta)$ is the steering vector of the receive array, $\mathbf{z}(t, \tau)$ is $N \times 1$ zero-mean white Gaussian noise term, and

$$r_l(t, \tau) \triangleq \sqrt{\frac{E}{M}} \alpha_l(\tau) \mathbf{a}^T(\theta_l) \boldsymbol{\phi}(t) \tag{3}$$

is the radar return due to the lth target. In (3), $\alpha_l(\tau)$, θ_l, and $\mathbf{a}(\theta_l)$ are the reflection coefficient with variance σ_α^2, spatial angle, and steering vector of the transmit array associated with the lth

target, respectively, $\boldsymbol{\phi}(t) \triangleq [\phi_1(t), \ldots, \phi_M(t)]^T$ is the waveform vector, and $(\cdot)^T$ stands for the transpose. Note that the reflection coefficient $\alpha_l(\tau)$ for each target is assumed to be constant during the whole pulse, but varies independently from pulse to pulse, i.e., it obeys the Swerling II target model [19].

Exploiting the orthogonality property of the transmitted waveforms, the $N \times 1$ component of the received data (2) due to the mth waveform can be extracted using matched-filtering which is given as follows

$$\mathbf{x}_m(\tau) \triangleq \int_T \mathbf{x}(t, \tau)\phi_m^*(t)dt, \quad m = 1, \ldots, M. \tag{4}$$

where $(\cdot)^*$ is the conjugation operator. Stacking the individual vector components (4) in one column vector, we obtain the $MN \times 1$ virtual data vector [3]

$$\begin{aligned} \mathbf{y}_{\text{MIMO}}(\tau) &\triangleq [\mathbf{x}_1^T(\tau) \cdots \mathbf{x}_M^T(\tau)]^T \\ &= \sqrt{\frac{E}{M}} \sum_{l=1}^{L} \alpha_l(\tau)\mathbf{a}(\theta_l) \otimes \mathbf{b}(\theta_l) + \tilde{\mathbf{z}}(\tau) \\ &= \sqrt{\frac{E}{M}} \sum_{l=1}^{L} \alpha_l(\tau)\mathbf{u}_{\text{MIMO}}(\theta_l) + \tilde{\mathbf{z}}(\tau) \end{aligned} \tag{5}$$

where $\otimes$ denotes the Kronker product,

$$\mathbf{u}_{\text{MIMO}}(\theta) \triangleq \mathbf{a}(\theta) \otimes \mathbf{b}(\theta) \tag{6}$$

is the $MN \times 1$ steering vector of the virtual array, and $\tilde{\mathbf{z}}(\tau)$ is the $MN \times 1$ noise term whose co-variance is given by $\sigma_z^2 \mathbf{I}_{MN}$. The $MN \times MN$ covariance matrix $\mathbf{R}_{\text{MIMO}} \triangleq \mathrm{E}\{\mathbf{y}_{\text{MIMO}}(\tau)\mathbf{y}_{\text{MIMO}}^H(\tau)\}$ is hard to obtain in practice. Therefore, the following sample covariance matrix

$$\hat{\mathbf{R}}_{\text{MIMO}} = \frac{1}{Q} \sum_{\tau=1}^{Q} \mathbf{y}_{\text{MIMO}}(\tau)\mathbf{y}_{\text{MIMO}}^H(\tau) \tag{7}$$

is used, where Q is the number of snapshots.

III. TRANSMIT BEAMSPACE BASED MIMO RADAR SIGNAL MODEL

Instead of transmitting omin-directionally, we propose to focus the transmitted energy within a sector $\boldsymbol{\Theta}$ by forming K directional beams where an independent waveform is transmitted over each beam. Note that the spatial sector $\boldsymbol{\Theta}$ can be estimated in a preprocessing step using any low-resolution DOA estimation technique of low complexity.

Let $\mathbf{C} \triangleq [\mathbf{c}_1, \ldots, \mathbf{c}_K]^T$ be the transmit beamspace matrix of dimension $M \times K$ ($K \leq M$), where $\mathbf{c}_k$ is the $M \times 1$ unit-norm weight vector used to form the kth beam. The beamspace matrix

can be properly designed to maintain constant beampattern within the sector of interest $\boldsymbol{\Theta}$ and to minimize the energy transmitted in the out-of-sector areas. Let $\boldsymbol{\phi}_K(t) \triangleq [\phi_1(t), \ldots, \phi_K(t)]^T$ be the $K \times 1$ waveform vector. The kth column of $\mathbf{C}$ is used to form a transmit beam for radiating the kth waveform $\phi_k(t)$. The signal radiated towards a hypothetical target located at a direction θ via the kth beam can be modeled as

$$s_k(t, \theta) = \sqrt{\frac{E}{K}} \left(\mathbf{c}_k^H \mathbf{a}(\theta) \right) \phi_k(t) \tag{8}$$

where $\sqrt{E/K}$ is a normalization factor used to satisfy the constraint that the total transmit energy is fixed to E. The signal radiated via all beams towards the direction θ can be modeled as

$$
\begin{aligned}
s(t, \theta) &= \sqrt{\frac{E}{K}} \sum_{k=1}^{K} \left(\mathbf{c}_k^H \mathbf{a}(\theta) \right) \phi_k(t) \\
&= \sqrt{\frac{E}{K}} \mathbf{C}^H \mathbf{a}(\theta) \boldsymbol{\phi}_K(t) = \sqrt{\frac{E}{K}} \tilde{\mathbf{a}}^T(\theta) \boldsymbol{\phi}_K(t)
\end{aligned} \tag{9}
$$

where $(\cdot)^H$ stands for the Hermitian transpose and

$$\tilde{\mathbf{a}}(\theta) \triangleq \left(\mathbf{C}^H \mathbf{a}(\theta) \right)^T. \tag{10}$$

Then, the transmit beamspace can be viewed as a transformation that results in changing the $M \times 1$ transmit array manifold $\mathbf{a}(\theta)$ into the $K \times 1$ manifold (10).

At the receive array, the $N \times 1$ complex vector of array observations can be expressed as

$$\mathbf{x}_{\text{beam}}(t, \tau) = \sqrt{\frac{E}{K}} \sum_{l=1}^{L} \alpha_l(\tau) \left(\tilde{\mathbf{a}}^T(\theta_l) \boldsymbol{\phi}_K(t) \right) \mathbf{b}(\theta_l) + \mathbf{z}(t, \tau). \tag{11}$$

By matched-filtering $\mathbf{x}_{\text{beam}}(t, \tau)$ to each of the waveforms ϕ_k $(k = 1, \ldots, K)$, the received signal component associated with each of the transmitted waveforms can be obtained as

$$
\begin{aligned}
\mathbf{y}_k(\tau) &\triangleq \int_T \mathbf{x}_{\text{beam}}(t, \tau) \phi_k^*(t) dt \\
&= \sqrt{\frac{E}{K}} \sum_{l=1}^{L} \alpha_l(\tau) \tilde{\mathbf{a}}_{[k]}(\theta_l) \mathbf{b}(\theta_l) + \mathbf{z}_k(\tau)
\end{aligned} \tag{12}
$$

where $(\cdot)_{[k]}$ is the kth entry of a vector and the $N \times 1$ noise term is defined as

$$\mathbf{z}_k(\tau) = \int_T \mathbf{z}(t, \tau) \phi_k^*(t) dt. \tag{13}$$

Stacking the individual vector components (12) in one column vector, we obtain the following $KN \times 1$ virtual data vector

$$\mathbf{y}_{\text{beam}}(\tau) \triangleq [\mathbf{y}_1^T(\tau) \cdots \mathbf{y}_K^T(\tau)]^T$$
$$= \sqrt{\frac{E}{K}} \sum_{l=1}^{L} \alpha_l(\tau) \left(\tilde{\mathbf{a}}(\theta_l) \otimes \mathbf{b}(\theta_l) \right) + \tilde{\mathbf{z}}_K(\tau) \quad (14)$$

where $\tilde{\mathbf{z}}_K(\tau) \triangleq [\mathbf{z}_1(\tau), \ldots, \mathbf{z}_K(\tau)]^T$ is the $KN \times 1$ noise term whose covariance is given by $\sigma_z^2 \mathbf{I}_{KN}$.

The transmit beamspace signal model given by (14) provides the basis for optimizing a general-shape transmit beampattern over the transmit beamspace weight matrix $\mathbf{C}$. By carefully designing $\mathbf{C}$, the transmitted energy can be focussed in a certain spatial sector, or divided between several disjoint sectors in space. As compared to traditional MIMO radar, the benefit of using transmit energy focusing is the possibility to increase in the signal power at each virtual array element. This increase in signal power is attributed to two factors:

(i) transmit beamforming gain, i.e., the signal power associated with the kth waveform reflected from a target at direction θ is magnified by factor $|\mathbf{c}_k^H \mathbf{a}(\theta)|^2$;

(ii) the signal power associated with the kth waveform is magnified by factor E/K due to dividing the fixed total transmit power E over $K \leq M$ waveforms instead of M waveforms.

As it is shown in subsequent sections, the aforementioned two factors result in increasing the SNR per virtual element which in turn results in lowering the CRB and improving the DOA estimation accuracy.

IV. TRANSMIT BEAMSPACE DESIGN

In this section, two methods for designing the transmit beamspace weight matrix $\mathbf{C}$ are proposed.

A. Motivations

Given the beamspace angular sector-of-interest $\boldsymbol{\Theta}$, several beamspace dimension reduction techniques applied to the data at the output of a passive receive array are reported in the literature (see [25] and references therein). The essence of these beamspace dimension reduction techniques is to perform DOA estimation in the reduced dimension space rather than in the elementspace (full dimension of received data) which leads to great computational savings. Performing DOA estimation in a reduced dimension beamspace has also proved to improve probability of source

resolution as well as estimation sensitivity [26]. However, it is well known that the CRB on DOA estimation performed in reduced dimension space is higher than (or at best equal to) the CRB on DOA estimation performed in elementspace, i.e., applying beamspace dimension reduction techniques to passive arrays does not improve the best achievable estimation performance [27]. This is natural because beamspace dimension reduction in passive arrays just preserves the signals observed within a certain spatial sector and filters out signals observed outside that sector.

The transmit beamspace processing proposed in Section III focuses all transmit energy within the desired spatial sector instead of spreading it omni-directionally in the whole spatial domain. In other words, the amount of energy that otherwise could be wasted in the out-of-sector areas is added to the amount of energy to be transmitted within the desired sector. As a result, the signal strength within the desired sector is increased potentially leading to improved best achievable estimation performance, i.e., as will be seen in Section VI-B lowering the CRB. The transmit beamspace weight matrix $\mathbf{C}$ can be designed such that the following two main requirement are satisfied: (i) Spatial distribution of energy transmitted within the desired sector is uniform; (ii) the amount of energy that is inevitably transmitted in the out-of-sector area is minimized. Here we present two methods for satisfying these two requirements.

B. Spheroidal Sequences Based Transmit Beamspace Design

Discrete prolate spheroidal sequences (DPSS) have been proposed for beamspace dimension reduction in array processing [28]. The essence of the DPSS-based approach to beamspace dimension reduction [21], [28] is to maximize the ratio of the beamspace energy that comes from within the desired sector $\boldsymbol{\Theta}$ to the total beamspace energy, i.e., the energy within the whole spatial domain $[-\pi/2, \ \pi/2]$. Following this principle, we propose to design the transmit beamspace weight matrix so that the ratio of the energy radiated within the desired spatial sector to the total radiated energy is maximized. That is, the transmit beamspace matrix $\mathbf{C}$ is designed based on maximizing

$$
\begin{aligned}
\Gamma_k &\triangleq \frac{\int_T \int_{\boldsymbol{\Theta}} \left| \mathbf{c}_k^H \mathbf{a}(\theta)\phi_k(t) \right|^2 d\theta dt}{\int_T \int_{-\frac{\pi}{2}}^{\frac{\pi}{2}} |\mathbf{c}_k^H \mathbf{a}(\theta)\phi_k(t)|^2 d\theta dt} \\
&= \frac{\mathbf{c}_k^H \left(\int_{\boldsymbol{\Theta}} \mathbf{a}(\theta)\mathbf{a}^H(\theta)d\theta \right) \mathbf{c}_k}{\int_{-\frac{\pi}{2}}^{\frac{\pi}{2}} |\mathbf{c}_k^H \mathbf{a}(\theta)|^2 d\theta} \\
&= \frac{\mathbf{c}_k^H \mathbf{A} \mathbf{c}_k}{\int_{-\frac{\pi}{2}}^{\frac{\pi}{2}} |\mathbf{c}_k^H \mathbf{a}(\theta)|^2 d\theta}
\end{aligned}
\tag{15}
$$

where $\mathbf{A} \triangleq \int_{\boldsymbol{\Theta}} \mathbf{a}(\theta)\mathbf{a}^H(\theta)d\theta$ is a non-negative matrix. Note that the first equality in (15) follows from the fact that $\int_T \phi(t)\phi^*(t)dt = 1$. Moreover, it can be shown that if $\mathbf{a}(\theta)$ obeys Vandermonde structure, then the following holds [21]

$$\int_{-\frac{\pi}{2}}^{\frac{\pi}{2}} |\mathbf{c}_k^H \mathbf{a}(\theta)|^2 d\theta = 2\pi \mathbf{c}_k^H \mathbf{c}_k. \tag{16}$$

Substituting (16) in (15), we obtain

$$\Gamma_k = \frac{\mathbf{c}_k^H \mathbf{A} \mathbf{c}_k}{2\pi \mathbf{c}_k^H \mathbf{c}_k}, \quad k = 1, \dots, K. \tag{17}$$

The maximization of the ration in (17) is equivalent to maximizing its numerator while fixing its denominator by imposing the constraint $\|\mathbf{c}_k\| = 1$. To avoid the trivial solution $\mathbf{c}_1 = \dots = \mathbf{c}_K$, an additional constraint might be necessary, for example, the orthogonality constraint $\mathbf{c}_k^H \mathbf{c}_{k'} = 0$, $k \neq k'$ can be imposed. Then, the maximization of $\{\Gamma_k\}_{k=1}^K$ subject to the constraint $\mathbf{C}^H \mathbf{C} = \mathbf{I}$ corresponds to finding the eigenvectors of $\mathbf{A}$ that are associated with the K largest eigenvalues of $\mathbf{A}$. That is, the transmit beamspace matrix is given as

$$\mathbf{C} = [\mathbf{u}_1, \mathbf{u}_2, \dots, \mathbf{u}_K] \tag{18}$$

where $\{\mathbf{u}_i\}_{i=1}^K$ are K principal eigenvectors of $\mathbf{A}$.

It is worth noting that any steering vector $\mathbf{a}(\theta), \theta \in \boldsymbol{\Theta}$ belongs to the space spanned by the columns of $\mathbf{C}$. This means that the magnitude of the projector of $\mathbf{a}(\theta)$ onto the column space of $\mathbf{C}$ is approximately constant, i.e., the transmit power distribution

$$H(\theta) = \mathbf{a}^H(\theta)\mathbf{C}\mathbf{C}^H\mathbf{a} \tag{19}$$

is approximately constant $\forall \theta \in \boldsymbol{\Theta}$. Therefore, the total transmit power distribution, i.e., the distribution of the power summed over all waveforms, within the spatial sector $\boldsymbol{\Theta}$ is approximately uniform. However, the transmit power distribution over individual waveforms may not be uniform within $\boldsymbol{\Theta}$. Such a uniform transmit power distribution over individual waveforms may be desired especially when the difference between the first and the last essential eigenvalues of $\mathbf{A}$ is significant. In this respect, note that the orthogonality constraint $\mathbf{C}^H \mathbf{C} = \mathbf{I}$ is imposed above only to avoid the trivial solution $\mathbf{c}_1 = \dots = \mathbf{c}_K$ when maximizing (17). This is different from the case of the traditional beamspace dimension reduction techniques where orthogonality is required to preserve the white noise property. Therefore, in our case where the latter is not an issue, $\mathbf{C}$ can be easily rotated, if necessary, so that it achieves desirable features such as uniform transmit power distribution over individual waveforms. The orthogonality may be lost

after such rotation of $\mathbf{C}$ without any consequences. For example, such rotation of $\mathbf{C}$ is used in our simulations (Section VII) to ensure that the uniform transmit power distribution per each individual waveform is achieved.

C. Convex Optimization Based Transmit Beamspace Design

A more general transmit beamspace design technique applicable to a transmit array of arbitrary geometry can also be formulated. Moreover, some DOA estimation techniques can be applied only if the received data enjoy certain properties. For example, the ESPRIT DOA estimation technique requires that the received data snapshots consist of two sets where one data set is equivalent to the other up to some phase rotation. This property is commonly referred to as rotational invariance. More generally, PARAFAC-based DOA estimation techniques are based on the assumption that multiple received data sets are related via rotational invariance properties. Fortunately, the transmit beamspace matrix $\mathbf{C}$ can be designed so that the virtual data vectors given by (12) enjoy such rotational invariance property.

To obtain the rotational invariance property, we propose a convex optimization based method for designing $\mathbf{C}$. For the virtual snapshots $\{\mathbf{y}_k(\tau)\}_{k=1}^{K}$ to enjoy rotational invariance, the following relationship should be satisfied

$$e^{\jmath\mu_k(\theta)} \left| \left(\mathbf{c}_k^H \mathbf{a}(\theta)\right) \right| \mathbf{b}(\theta) = e^{\jmath\mu_{k'}(\theta)} \left| \left(\mathbf{c}_{k'}^H \mathbf{a}(\theta)\right) \right| \mathbf{b}(\theta), \quad \forall \theta \in \mathbf{\Theta}, \quad k, k' = 1, \ldots, K \tag{20}$$

where $\jmath \triangleq \sqrt{-1}$, and $\mu_k(\theta)$ and $\mu_{k'}(\theta)$ are arbitrary phase shifts associated with the kth and k'th virtual snapshots, respectively. The relationship (20) can be satisfied if the transmit beamspace matrix $\mathbf{C}$ is designed/optimized to meet the following requirement

$$\mathbf{C}^H \mathbf{a}(\theta) = \mathbf{d}(\theta), \quad \forall \theta \in \mathbf{\Theta}. \tag{21}$$

where $\mathbf{d}(\theta) \triangleq [e^{\jmath\mu_1(\theta)}, \ldots, e^{\jmath\mu_K(\theta)}]^T$ is of dimension $K \times 1$. A meaningful formulation of a corresponding optimization problem is to minimize the norm of the difference between the left- and right-hand sides of (21) while keeping the worst transmit power distribution in the out-of-sector area below a certain level. This can be mathematically expressed as follows

$$\min_{\mathbf{C}} \max_i \|\mathbf{C}^H \mathbf{a}(\theta_i) - \mathbf{d}(\theta)\|, \quad \theta_i \in \mathbf{\Theta}, \quad i = 1, \ldots, I \tag{22}$$

$$\text{subject to} \quad \|\mathbf{C}^H \mathbf{a}(\theta_j)\| \leq \gamma, \quad \theta_j \in \bar{\mathbf{\Theta}}, \quad j = 1, \ldots, J \tag{23}$$

where $\bar{\mathbf{\Theta}}$ combines a continuum of all out-of-sector directions, i.e., directions lying outside the sector-of-interest $\mathbf{\Theta}$, and $\gamma > 0$ is the parameter of the user choice that characterizes the worst

acceptable level of transmit power radiation in the out-of-sector region. The parameter γ has an analogy to the stop-band attenuation parameters in the classic bandpass filter design and can be chosen in a similar fashion [29].

V. TRANSMIT BEAMSPACE BASED DOA ESTIMATION

In this section, we design DOA estimation methods based on transmit beamspace processing in MIMO radar. We focus on subspace based DOA estimation techniques such as MUSIC and ESPRIT.

A. Transmit Beamspace Based MUSIC

The virtual data model (14) can be rewritten as

$$\mathbf{y}_{\text{beam}}(\tau) = \mathbf{V}\boldsymbol{\alpha}(\tau) + \tilde{\mathbf{z}}_K(\tau) \tag{24}$$

where

$$\boldsymbol{\alpha}(\tau) \triangleq [\alpha_1(\tau), \ldots, \alpha_L(\tau)]^T \tag{25}$$

$$\mathbf{V} \triangleq [\mathbf{v}(\theta_1), \ldots, \mathbf{v}(\theta_L)] \tag{26}$$

$$\mathbf{v}(\theta) \triangleq \sqrt{\frac{E}{K}} \left(\mathbf{C}^H \mathbf{a}(\theta) \right) \otimes \mathbf{b}(\theta). \tag{27}$$

The $KN \times KN$ transmit beamspace-based covariance matrix is given by

$$\mathbf{R}_{\text{beam}} \triangleq \text{E} \left\{ \mathbf{y}_{\text{beam}}(\tau)\mathbf{y}_{\text{beam}}^H(\tau) \right\}$$

$$= \mathbf{V}\mathbf{S}\mathbf{V}^H + \sigma_z^2 \mathbf{I}_{KN} \tag{28}$$

where $\mathbf{S} \triangleq \text{E}\{\boldsymbol{\alpha}(\tau)\boldsymbol{\alpha}^H(\tau)\}$ is the covariance matrix of the reflection coefficients vector. The sample estimate of (28) takes the following form

$$\hat{\mathbf{R}}_{\text{beam}} = \frac{1}{Q} \sum_{\tau=1}^{Q} \mathbf{y}_{\text{beam}}(\tau)\mathbf{y}_{\text{beam}}^H(\tau). \tag{29}$$

The eigendecomposition of (29) can be written as

$$\hat{\mathbf{R}}_{\text{beam}} = \mathbf{E}_s \boldsymbol{\Lambda}_s \mathbf{E}_s^H + \mathbf{E}_n \boldsymbol{\Lambda}_n \mathbf{E}_n^H \tag{30}$$

where the $L \times L$ diagonal matrix $\boldsymbol{\Lambda}_s$ contains the largest (signal-subspace) eigenvalues and the columns of the $KN \times L$ matrix $\mathbf{E}_s$ are the corresponding eigenvectors. Similarly, the $(KN - L) \times (KN - L)$ diagonal matrix $\boldsymbol{\Lambda}_n$ contains the smallest (noise-subspace) eigenvalues while the $KN \times (KN - L)$ matrix $\mathbf{E}_n$ is built from the corresponding eigenvectors.

Applying the principle of the elementspace MUSIC estimator [5], the transmit beamspace spectral-MUSIC estimator can be expressed as

$$f(\theta) = \frac{\mathbf{v}^H(\theta)\mathbf{v}(\theta)}{\mathbf{v}^H(\theta)\mathbf{Q}\mathbf{v}(\theta)} \tag{31}$$

where $\mathbf{Q} = \mathbf{E}_{\mathrm{n}}\mathbf{E}_{\mathrm{n}}^H = \mathbf{I} - \mathbf{E}_{\mathrm{s}}\mathbf{E}_{\mathrm{s}}^H$ is the projection matrix onto the noise subspace. Substituting (27) into (31), we obtain

$$
\begin{aligned}
f(\theta) &= \frac{\left[(\mathbf{C}^H\mathbf{a}(\theta)) \otimes \mathbf{b}(\theta)\right]^H \left[(\mathbf{C}^H\mathbf{a}(\theta)) \otimes \mathbf{b}(\theta)\right]}{\left[(\mathbf{C}^H\mathbf{a}(\theta)) \otimes \mathbf{b}(\theta)\right]^H \mathbf{Q}\left[(\mathbf{C}^H\mathbf{a}(\theta)) \otimes \mathbf{b}(\theta)\right]} \\
&= \frac{\left[\mathbf{a}^H(\theta)\mathbf{C}\mathbf{C}^H\mathbf{a}(\theta)\right] \cdot \left[\mathbf{b}^H(\theta)\mathbf{b}(\theta)\right]}{\left[(\mathbf{C}^H\mathbf{a}(\theta)) \otimes \mathbf{b}(\theta)\right]^H \mathbf{Q}\left[(\mathbf{C}^H\mathbf{a}(\theta)) \otimes \mathbf{b}(\theta)\right]} \\
&= \frac{N\mathbf{a}^H(\theta)\mathbf{C}\mathbf{C}^H\mathbf{a}(\theta)}{\left[(\mathbf{C}^H\mathbf{a}(\theta)) \otimes \mathbf{b}(\theta)\right]^H \mathbf{Q}\left[(\mathbf{C}^H\mathbf{a}(\theta)) \otimes \mathbf{b}(\theta)\right]}.
\end{aligned} \tag{32}
$$

B. Transmit Beamspace Based ESPRIT

The signal component of the data vectors $\{\mathbf{y}_k(\tau)\}_{k=1}^K$ can be expressed as

$$\mathbf{y}_k(\tau) = \mathbf{T}_k\boldsymbol{\alpha}(\tau) \tag{33}$$

where

$$\mathbf{T}_k \triangleq [\mathbf{b}(\theta_1), \ldots, \mathbf{b}(\theta_L)]\boldsymbol{\Psi}_k \tag{34}$$

$$\boldsymbol{\Psi}_k \triangleq \mathrm{diag}\left\{\mathbf{c}_k^H\mathbf{a}(\theta_1), \ldots, \mathbf{c}_k^H\mathbf{a}(\theta_L)\right\}. \tag{35}$$

It is worth noting that the matrices $\{\mathbf{T}_k\}_{k=1}^K$ are related to each other as

$$\mathbf{T}_k = \mathbf{T}_j\boldsymbol{\Psi}_j^{-1}\boldsymbol{\Psi}_k, \quad k, j = 1, \ldots, K. \tag{36}$$

By carefully designing the beamspace weight matrix $\mathbf{C}$, for example by using (22)–(23), the relationship (36) enjoys the rotational invariance property.

Consider the case when only two transmit beams are formed. Then, the transmit beamspace matrix is $\mathbf{C} = [\mathbf{c}_1, \mathbf{c}_2]$. In this case, (36) simplifies to

$$\mathbf{T}_2 = \mathbf{T}_1\boldsymbol{\Psi} \tag{37}$$

where

$$\boldsymbol{\Psi} \triangleq \mathrm{diag}\left\{\frac{\mathbf{c}_2^H\mathbf{a}(\theta_1)}{\mathbf{c}_1^H\mathbf{a}(\theta_1)}, \ldots, \frac{\mathbf{c}_2^H\mathbf{a}(\theta_L)}{\mathbf{c}_1^H\mathbf{a}(\theta_L)}\right\}. \tag{38}$$

Furthermore, (38) can be rewritten as

$$\boldsymbol{\Psi} = \mathrm{diag}\left\{A(\theta_1)e^{j\Omega(\theta_1)}, \ldots, A(\theta_L)e^{j\Omega(\theta_L)}\right\} \tag{39}$$

where $A(\theta)$ and $\Omega(\theta)$ are the magnitude and angle of $\mathbf{c}_2^H \mathbf{a}(\theta)/\mathbf{c}_1^H \mathbf{a}(\theta)$, respectively. It can be seen from (37) and (39) that the vectors $\mathbf{y}_1$ and $\mathbf{y}_2$ (see also (33)) enjoy the rotational invariance property. Therefore, ESPRIT-based DOA estimation techniques can be used to estimate $\boldsymbol{\Psi}$ and $\{\theta_l\}_{l=1}^L$ can be obtained from $\boldsymbol{\Psi}$ by looking up a table that converts $\Omega(\theta)$ to θ. Moreover, if $K > 2$ is chosen, more than two data sets which enjoy the rotational invariance property can be obtained by properly designing the transmit beamspace weight matrix. In this case, the means of using PARAFAC instead of ESPRIT are provided as well.

It is worth mentioning that for traditional MIMO radar (5), DOA estimation using ESPRIT has been proposed in [17]. Specifically, $\mathbf{y}(\tau)$ in (5) has been partitioned into $\mathbf{y}_1(\tau) \triangleq [\mathbf{x}_1^T(\tau),$ $\ldots, \mathbf{x}_{M-1}^T(\tau)]^T$ and $\mathbf{y}_2(\tau) \triangleq [\mathbf{x}_2^T(\tau), \ldots, \mathbf{x}_M^T(\tau)]^T$ and it has been shown that $\mathbf{y}_1$ and $\mathbf{y}_2$ obey the rotational invariance property which enables the use of ESPRIT for DOA estimation. However, the rotational invariance property is valid in [17] only when the transmit array is a uniform linear array (ULA). Therefore, the method of [17] is limited by the transmit array structure and may suffer from performance degradation in the presence of array perturbation errors. Moreover, it suffers from low SNR per virtual antenna as a result of dividing the total transmit energy over M different waveforms.

VI. PERFORMANCE ANALYSIS

In this section, we analyze the performance of the proposed transmit beamspace MIMO radar DOA estimation approach as compared to the MIMO radar DOA estimation technique. For the reason of comparison, we also consider two techniques that have been recently reported in the literature that employ the idea of dividing the transmit array into several smaller sub-apertures/subarrays. The first technique uses transmit subapertures (TS) for omni-directionally radiating independent waveforms [30], [31]. If the number of subapertures is chosen as $K < M$, then each subaperture radiates pulses of energy E/K. The second technique is based on partitioning the transmit array into overlapped subarrays where the antennas that belong to each subarray are used to coherently transmit an independent waveform [22], [23]. We refer to this technique as transmit array partitioning (TAP). Note that the TAP technique has transmit coherent gain while the TS technique does not have such a coherent transmit gain.

In the following subsection, we compare between the aforementioned techniques in terms of the effective aperture of the corresponding virtual array, the SNR gain per virtual element, and the computational complexity associated with eigendecomposition based DOA estimation

techniques. In the next subsection, we express/discuss the CRB for all considered techniques.

A. Colocated Uniform Linear Transmit Array

Consider the case of a ULA at the transmitter with $\lambda/2$ spacing between adjacent antennas, where λ is the propagation wavelength. Taking the first antenna as a reference, the transmit steering vector can be expressed as

$$\mathbf{a}(\theta) \triangleq \left[1, e^{-j\pi\sin\theta}, \ldots, e^{-j\pi(M-1)\sin\theta}\right]^T. \tag{40}$$

Also, the receive antennas are assumed to be grouped in a ULA with half a wavelength interelement spacing. Then, the receive steering vector is given as

$$\mathbf{b}(\theta) \triangleq \left[1, e^{-j\pi\sin\theta}, \ldots, e^{-j\pi(N-1)\sin\theta}\right]^T. \tag{41}$$

It is worth noting that the transmit and receive array apertures are $(M-1)\lambda/2$ and $(N-1)\lambda/2$, respectively. In light of (40) and (41), we discuss/analyze the following cases.

1) Traditional MIMO radar: Substituting (40) and (41) in (6), the MIMO radar virtual steering vector can be expressed as

$$\mathbf{u}_{\text{MIMO}}(\theta) = \left[1, \ldots, e^{-j\pi(N-1)\sin\theta}, e^{-j\pi\sin\theta}, \ldots, e^{-j\pi N\sin\theta}, \right.$$
$$\left. \ldots, e^{-j\pi(M-1)\sin\theta}, \ldots, e^{-j2\pi(M-1+N-1)\sin\theta}\right]^T. \tag{42}$$

From (42), we observe that the effective virtual array aperture is $(M+N-2)\lambda/2$. Note that the virtual steering vector $\mathbf{a}(\theta) \otimes \mathbf{a}(\theta)$ is of dimension $MN \times 1$, yet it only contains $M+N-1$ distinct elements. Moreover, the SNR gain per virtual element is proportional in this case to E/M. This low SNR gain can lead to poor DOA estimation performance especially at low SNR region. The computational complexity of applying eigen-decomposition based DOA estimation techniques is of $O(M^3N^3)$ in this case.

2) Transmit subaperturing based MIMO radar: As compared to the traditional MIMO radar, TS-based MIMO radar employs K subapertures instead of M. This results in higher SNR per virtual element in the corresponding virtual array at the receiver. To capitalize on the effect of this factor on the DOA estimation performance, we consider the extreme case when only two transmit subapertures[2] are used to radiate the total transmit energy E. In this case, each transmit

---

[2]One can think of a subaperture as a large omni-directional antenna which is capable of radiating energy $E/2$ instead of E/M. This case might be practically unattractive as it will require power amplifier of much higher amplifying gain as compared to the case of using M transmit antennas. However, for the sake of theoretical analysis/comparison we consider it in this paper.

subaperture radiates a waveform of energy $E/2$. Assume that the two transmit subapertures are separated in space by ζ wavelength and that the first transmit subaperture is taken as a reference. Then, the MIMO radar data model (5) becomes of dimension $2N \times 1$ and can be expressed as

$$\mathbf{y}_{\mathrm{TS}}(\tau) = \sqrt{\frac{E}{2}} \sum_{l=1}^{L} \alpha_l(\tau) \left([1, \ e^{-j2\pi\zeta\sin\theta_l}]^T \otimes \mathbf{b}(\theta)\right) + \tilde{\mathbf{z}}_{\mathrm{TS}}(\tau) \tag{43}$$

where $\tilde{\mathbf{z}}_{\mathrm{TS}}(\tau) = [\mathbf{z}_1(\tau), \ \mathbf{z}_2(\tau)]^T$.

Comparing (5) to (43), we observe that the signal strength for MIMO radar with M transmit antennas is proportional to $\sqrt{E/M}$ while the signal strength for the TS-based MIMO radar is proportional to $\sqrt{E/2}$. This means that (43) offers an SNR gain that is $M/2$ times the SNR gain offered by (5). We also observe from (43) that the effective virtual array aperture is given by $(\zeta + N - 1)\lambda/2$. Therefore, the effective aperture for this case can be controlled by selecting ζ. For example, selecting $\zeta = \lambda/2$ yields a virtual array steering vector of dimension $2N$ that contains only $N + 1$ distinct elements, i.e, the effective aperture would be $N\lambda/2$. This case is particularly important when performing DOA estimation using search free techniques such as ESPRIT. Another important case is the choice $\zeta = N\lambda/2$ which yields a virtual array that is equivalent to a $2N$-element ULA. In this case, the effective array aperture will be $(2N - 1)\lambda/2$. The computational complexity of applying eigen-decomposition based DOA estimation techniques is of $O(2^3 N^3)$ in this case.

3) Transmit array partitioning based MIMO radar: Following the guidelines of [23] and selecting $K = 2$, the M-antenna transmit array is assumed to be partitioned into two fully overlapped subarrays of $M - 1$ antenna each. The $(M - 1) \times 1$ beamforming weight vectors $\mathbf{w}_1 = \mathbf{w}_2 = \mathbf{w}$ are used to form transmit beams that cover the spatial sector Θ. Two independent waveforms are radiated. Each waveform has $E/2$ energy per pulse. The transmit weight vector $\mathbf{w}$ can be designed such that the transmit gain is approximately the same within the desired sector Θ, i.e., $|\mathbf{w}^H \bar{\mathbf{a}}(\theta)| = G_{\mathrm{TAP}}$, $\forall\theta \in \Theta$ where $\bar{\mathbf{a}}(\theta)$ contains the first $M - 1$ elements of the vector $\mathbf{a}(\theta)$ and G_{TAP} is the TAP transmit coherent processing gain. Then, the TAP-based MIMO radar data model becomes of dimension $2N \times 1$ and can be formally expressed as

$$\mathbf{y}_{\mathrm{TAP}}(\tau) = \sqrt{\frac{E}{2}} \sum_{l=1}^{L} \alpha_l(\tau) \left(\mathbf{w}^H \bar{\mathbf{a}}(\theta_l)\right) \mathbf{u}_{\mathrm{TAP}}(\theta_l) + \tilde{\mathbf{z}}_{\mathrm{TAP}}(\tau)$$

$$= G_{\mathrm{TAP}} \sqrt{\frac{E}{2}} \sum_{l=1}^{L} \alpha_l(\tau) \mathbf{u}_{\mathrm{TAP}}(\theta_l) + \tilde{\mathbf{z}}_{\mathrm{TAP}}(\tau) \tag{44}$$

where $\mathbf{u}_{\text{TAP}}(\theta) \triangleq [1, \ e^{-j\pi \sin \theta}]^T \otimes \mathbf{b}(\theta)$ is the $2N \times 1$ steering vector of the corresponding virtual array. Note that the TAP-based MIMO radar has transmit coherent gain G_{TAP} which results in improvement in SNR per virtual element. However, the corresponding virtual array contains $N+1$ distinct elements, i.e., the effective virtual array aperture is limited to $N\lambda/2$. The computational complexity of applying eigen-decomposition based DOA estimation techniques is of $O(2^3 N^3)$ in this case.

4) Transmit beamspace based MIMO radar: For the proposed transmit beamspace MIMO radar, we choose $K = 2$ and use (22)–(23) for designing $\mathbf{C} = [\mathbf{c}_1 \ \mathbf{c}_2]$ such that

$$\mathbf{d}(\theta) = G_{\text{beam}} \cdot [1, \ e^{-j2\pi N \sin \theta}]^T, \quad \forall \theta \in \mathbf{\Theta} \tag{45}$$

where G_{beam} is the transmit beamspace gain, i.e., $|\mathbf{c}_1^H \mathbf{a}(\theta)| \approx |\mathbf{c}_2^H \mathbf{a}(\theta)| \approx G_{\text{beam}}, \ \forall \theta \in \mathbf{\Theta}$. This yields a virtual array with $2N$ distinct elements and $(2N-1)\lambda/2$ effective array aperture. Moreover, the proposed transmit beamspace technique offers SNR gain of $G_{\text{beam}} \cdot E/M$, i.e., it combines all the benefits of all other aforementioned techniques. The computational complexity of applying eigen-decomposition based DOA estimation techniques is of $O(2^3 N^3)$ in this case.

A comparison between all methods considered is summarized in the following table.

Table1: Comparison between transmit beamspace-based MIMO radar and other existing techniques.

	Effective aperture	SNR gain per virtual element	Computational complexity
Traditional MIMO (5)	$(M + N - 2)\frac{\lambda}{2}$	$\frac{E}{M}$	$O(M^3 N^3)$
Transmit subaperturing ($\zeta = \frac{\lambda}{2}$)	$N\frac{\lambda}{2}$	$\frac{E}{2}$	$O(2^3 N^3)$
Transmit subaperturing ($\zeta = N\frac{\lambda}{2}$)	$(2N - 1)\frac{\lambda}{2}$	$\frac{E}{2}$	$O(2^3 N^3)$
Transmit array partitioning (44)	$N\frac{\lambda}{2}$	$G_{\text{TAP}}^2 \cdot \frac{E}{2}$	$O(2^3 N^3)$
Transmit beamspace MIMO (45)	$(2N - 1)\frac{\lambda}{2}$	$G_{\text{beam}}^2 \cdot \frac{E}{2}$	$O(2^3 N^3)$

B. Cramér-Rao Bound

In this section, we discuss the CRB on DOA estimation accuracy in transmit beamspace-based MIMO radar.

In the case of transmit beamspace-based MIMO radar, the virtual data model (14) satisfies the following statistical model:

$$\mathbf{y}_{\text{beam}}(\tau) \sim \mathcal{N}_C \left(\boldsymbol{\mu}(\tau), \mathbf{R} \right) \tag{46}$$

where $\mathcal{N}_C$ denotes the complex multivariate circularly Gaussian probability density function, $\boldsymbol{\mu}(\tau)$ is the mean of $\mathbf{y}_{\text{beam}}(\tau)$, and $\mathbf{R}$ is its covariance matrix.

1) Stochastic CRB: The stochastic CRB on estimating the DOAs using the data model (14) is derived by assuming $\boldsymbol{\mu}(\tau) = \mathbf{0}$ and $\mathbf{R} = \mathbf{R}_{\text{beam}}$, where $\mathbf{R}_{\text{beam}}$ is given by (28). Note that under these assumptions, the virtual array signal model (14) (or its equivalent representation (24)) has the same form as the signal model used in [32] to derive the stochastic CRB for DOA estimation in conventional array processing. Therefore, the CRB expressions in its general form derived in [32] can be used for computing the stochastic CRB for estimating the DOAs based on (24), that is,

$$\text{CRB}(\theta) = \frac{\sigma_z^2}{2Q} \left\{ \text{Re}(\mathbf{D}\mathbf{P}_\mathbf{V}^\perp \mathbf{D}) \odot \mathbf{G}^T \right\}^{-1} \tag{47}$$

where $\mathbf{P}_\mathbf{V}^\perp \triangleq \mathbf{V}(\mathbf{V}^H\mathbf{V})^{-1}\mathbf{V}^H$ is the projection matrix onto the space spanned by the columns of $\mathbf{V}$, and $\mathbf{G} \triangleq (\mathbf{S}\mathbf{V}^H\mathbf{R}^{-1}\mathbf{V}\mathbf{S})$. In (47), $\mathbf{D} \triangleq [\mathbf{d}(\theta_1), \dots, \mathbf{d}(\theta_L)]$ is the matrix whose lth column is given by the derivative of the lth column of $\mathbf{V}$ with respect to θ_l, i.e.,

$$\mathbf{d}(\theta) \triangleq \frac{d\mathbf{v}(\theta)}{d\theta} = \sqrt{\frac{E}{K}} \frac{d\left[(\mathbf{C}^H\mathbf{a}(\theta)) \otimes \mathbf{b}(\theta)\right]}{d\theta}$$
$$= \sqrt{\frac{E}{K}} \left((\mathbf{C}^H\mathbf{a}'(\theta)) \otimes \mathbf{b}(\theta) + (\mathbf{C}^H\mathbf{a}(\theta)) \otimes \mathbf{b}'(\theta)\right) \tag{48}$$

where $\mathbf{a}'(\theta) = d\mathbf{a}(\theta)/d\theta$ and $\mathbf{b}'(\theta) = d\mathbf{b}(\theta)/d\theta$.

2) Deterministic CRB: The deterministic CRB is derived by assuming $\boldsymbol{\mu}(\tau) = \mathbf{V}\boldsymbol{\alpha}(\tau)$ and $\mathbf{R} = \sigma_z^2\mathbf{I}_{KN}$. Under these statistical assumptions, the virtual data model (14) is similar to the general model used in [33] to find the deterministic CRB. According to [33], the deterministic CRB expression can be obtained from (47) by replacing $\mathbf{G}$ with $\hat{\mathbf{S}}$, where $\hat{\mathbf{S}}$ is the sample estimate of $\mathbf{S}$.

It is worth noting that the expression (47) can be used not only for computing the CRB for the proposed transmit beamspace technique but also for the other techniques summarized in Table 1. Indeed, the following cases show how these techniques can be viewed as special cases of the proposed model (14).

1) Choosing $\mathbf{C} = \mathbf{I}_M$, the transmit beamspace signal model (14) simplifies to the traditional MIMO radar signal model (5). Therefore, the CRB for the traditional MIMO radar can be obtained by substituting $\mathbf{C} = \mathbf{I}_M$ in (47) and (48).

2) The TS-based MIMO radar signal model with $\zeta = \lambda/2$ can be obtained from (14) by

choosing $\mathbf{C}$ in the following format

$$\mathbf{C} = \begin{bmatrix} 1 & 0 & \mathbf{0} \\ 0 & 1 & \mathbf{0} \end{bmatrix}^T. \tag{49}$$

3) The TS-based MIMO radar signal modal for $\zeta = N\lambda/2$ can be obtained from (14) by choosing $\mathbf{C}$ in the following format

$$\mathbf{C} = \begin{bmatrix} 1 & \mathbf{0} & 0 \\ 0 & \mathbf{0} & 1 \end{bmatrix}^T. \tag{50}$$

4) Finally, the TAP-based MIMO radar signal model (44) can be obtained from (14) by choosing $\mathbf{C}$ in the following format

$$\mathbf{C} = \begin{bmatrix} \mathbf{w}_1 & 0 \\ 0 & \mathbf{w}_2 \end{bmatrix}. \tag{51}$$

VII. SIMULATION RESULTS

Throughout our simulations, we assume a uniform linear transmit array of $M = 10$ omni-directional antennas spaced half a wavelength apart. At the receiver, $N = 10$ omni-directional antennas are also assumed. The additive noise is Gaussian zero-mean unit-variance spatially and temporally white. Two targets are located at directions $-1°$ and $1°$, respectively. The sector of interest $\mathbf{\Theta} = [-5°, 5°]$ is taken. Several examples are used to compare the performances of the following methods: (i) The traditional MIMO radar (5); (ii) The TS-based MIMO radar (49) with $\zeta = \lambda/2$; (iii) The TS-based MIMO radar (49) with $\zeta = N\lambda/2$; (iv) the TAP-based MIMO radar (51); and (v) The proposed transmit beamspace MIMO radar (14). For all methods tested, the total transmit energy is fixed to $E = M$. For the traditional MIMO radar (5), each transmit antenna is used for omni-directional radiation of one of the baseband waveforms

$$\phi_m(t) = \sqrt{\frac{1}{T}} e^{j2\pi\frac{m}{T}t}, \quad m = 1, \ldots, M. \tag{52}$$

For all methods that radiate two waveforms only, the first and second waveforms of (52) are used. The total number of virtual snapshots used to compute the sample covariance matrix is $Q = 300$. In all examples, the RMSEs and the probability of source resolution for all methods tested are computed based on 500 independent runs.

A. Example 1: Stochatstic and Deterministic CRBs

For the proposed spheroidal sequences based transmit beamspace MIMO radar (18), the non-negative matrix $\mathbf{A} = \int_{\boldsymbol{\Theta}} \mathbf{a}(\theta)\mathbf{a}^H(\theta)d\theta$ is built. The two eigenvectors associated with the largest two eigenvalues are taken as the principle eigenvectors, i.e., $\mathbf{C} = [\mathbf{u}_1 \ \mathbf{u}_2]$ is used. Two waveforms are assumed to be radiated where each column of $\mathbf{C}$ is used to form a transmit beam for radiating a single waveform. Fig. 1 shows the transmit power distribution of the individual waveforms $|\mathbf{c}_k\mathbf{a}(\theta)|^2$, $k = 1, 2$ as well as the distribution of the total transmitted power (19). As we can see from this figure, the individual waveform power is not uniformly distributed within the sector $\boldsymbol{\Theta}$ while the distribution of the total transmitted power is uniform. To achieve uniform transmit power distribution for each waveform a simple modification that involves vector rotation to the transmit beamspace matrix $\mathbf{C}$ can be performed. This means that $\mathbf{C}$ can be modified as

$$\tilde{\mathbf{C}} = \mathbf{C}\mathbf{Q} \tag{53}$$

where $\mathbf{Q}$ is a 2×2 unitary matrix defined as

$$\mathbf{Q} = \begin{bmatrix} \sqrt{1/2} & \sqrt{1/2} \\ \sqrt{1/2} & -\sqrt{1/2} \end{bmatrix}. \tag{54}$$

Fig. 2 shows the transmit power distribution for the individual waveforms $|\tilde{\mathbf{c}}_k\mathbf{a}(\theta)|^2$, $k = 1, 2$ as well as for the total transmitted power (19). It can be seen from this figure that the distribution of individual waveforms is uniform within the desired sector.

For the TAP-based method, the transmit array is partitioned into two overlapped subarrays of 9 antennas each. Each subarray is used to focus the radiation of one waveform within the sector $\boldsymbol{\Theta}$. The transmit weight vectors are chosen as $\mathbf{w}_1 = \mathbf{w}_2 = [-0.5623 \ -0.5076 \ -0.4358$ $-0.3501 \ -0.2542 \ -0.1524 \ -0.0490 \ 0.0512 \ 0.1441]^T$. This specific selection is obtained by averaging the two eigenvectors associated with the maximum two eignevalues of the matrix $\int_{\boldsymbol{\Theta}} \mathbf{a}_1(\theta)\mathbf{a}_1^H(\theta)d\theta$, where $\mathbf{a}_1(\theta)$ is the 9×1 steering vector associated with the first subarray.[3] The transmit power distribution of both waveforms is exactly the same as shown in Fig. 3.

The stochastic CRBs for all methods considered are plotted versus $\mathrm{SNR} = \sigma_\alpha^2/\sigma_z^2$ in Fig. 4. It can be seen from this figure that the TS-based MIMO radar with $\zeta = \lambda/2$ has the highest/worst CRB as compared to all other methods. Its poor CRB performance is attributed to the omni-directional transmission, i.e., wasting a considerable fraction of the transmitted energy within

---

[3]Note that if the transmit array is not a ULA, then $\mathbf{w}_1$ and $\mathbf{w}_2$ can be designed independently using classic FIR filter design techniques.

the out-of-sector region, and to the small effective aperture of the corresponding virtual array. We can also see from the figure that the TS-based MIMO radar with $\zeta = N\lambda/2$ exhibits much lower stochastic CRB as compared to the case with $\zeta = \lambda/2$. The reason for this improvement is the larger effective aperture of the corresponding virtual array. The traditional MIMO radar with M transmit antennas has the same effective aperture as that of the TS-based MIMO radar with $\zeta = N\lambda/2$ but lower SNR per virtual element. Therefore, the stochastic CRB for traditional MIMO radar is higher than the CRB for the TS-based MIMO radar with $\zeta = N\lambda/2$. At the same time, it is better than the CRB of the TS-based MIMO radar with $\zeta = \lambda/2$ due to larger effective aperture. The TAP-based MIMO radar has the same effective aperture as that of the TS-based MIMO radar with $\zeta = \lambda/2$ but higher SNR per virtual element due to transmit coherent processing gain. It yields lower CRB. In fact, the CRB for the TAP-based MIMO radar is comparable to that of the traditional MIMO radar. Finally, the transmit beamspace MIMO radar with spheroidal sequences based transmit weight matrix has the lowest CRB as compared to all other methods. This can be attributed to the fact that the proposed transmit beamspace-based MIMO radar combines the benefits of having high SNR due to energy focusing, high power of individual waveforms, and large effective aperture of the corresponding virtual array.

The deterministic CRBs for all methods considered are plotted in Fig. 5. As can be seen from this figure, the same observations and conclusion that are drawn from the stochastic CRB curves also apply to the deterministic CRB.

B. Example 2: MUSIC-based DOA Estimation

In this example, the MUSIC algorithm is used to estimate the DOA for all aforementioned methods. Note that the targets are considered to be resolved if there are at least two peaks in the MUSIC spectrum and the following is satisfied [21]

$$\left|\hat{\theta}_l - \theta_l\right| \leq \frac{\Delta\theta}{2}, \quad l = 1, 2 \tag{55}$$

where $\Delta\theta = |\theta_2 - \theta_1|$. Fig. 6 shows the probability of source resolution versus SNR for all methods tested. It can be seen from this figure that all methods exhibit a 100% correct source resolution at high SNR values. As the SNR decreases, the probability of source resolution starts dropping for each method at a certain point until it eventually becomes zero. The SNR level at which this transition happens is known as SNR threshold. It can be seen from Fig. 6 that the TS-based MIMO radar with $\zeta = \lambda/2$ has the highest SNR threshold while the traditional

MIMO radar and the TAP-based MIMO radar have the second and third highest SNR thresholds, respectively. The SNR threshold of the TS-based MIMO radar with $\zeta = N\lambda/2$ is lower than the aforementioned three methods while the proposed transmit beamspace-based MIMO radar has the lowest SNR threshold, i.e., the best probability of source resolution performance.

Fig. 7 shows the RMSEs for the MUSIC-based DOA estimators versus SNR for all methods tested. It can be seen from this figure that the TS-based MIMO radar with $\zeta = \lambda/2$ has the highest/poorest RMSE performance. It can also be seen that the TAP-based MIMO radar outperforms the traditional MIMO radar at low SNR region while the opposite occurs at high SNR region. This means that the influence of having large effective aperture is prominent at high SNR region, while the benefit of having high SNR gain per virtual antenna (even if the effective aperture is small) is feasible at low SNR region. It can also be observed from Fig. 7 that the estimation performance of the TS-based MIMO radar with $\zeta = N\lambda/2$ is better than that of both the traditional MIMO radar and the TAP-based MIMO radar. Finally, the proposed transmit beamspace-based MIMO radar outperforms all aforementioned methods.

It is worth noting that the width of the desired sector is $10°$. Therefore, the parts of the RMSE curves where the RMSEs exceed $10°$ in Fig. 7 are not important. Thus, the comparison between different methods within that region is meaningless.

C. Example 3: ESPRIT-based DOA Estimation

In this example, all parameters for all methods are the same as in the previous example except for the $M \times 2$ transmit weight matrix associated with transmit beamspace-based MIMO radar which is designed using (22)–(23). The out-of-sector region is taken as $\bar{\Theta} = [-90°, -15°] \cup [15°, 90°]$ and the parameter that controls the level of radiation within $\bar{\Theta}$ is taken as $\gamma = 0.38$. Each column of the resulting matrix $\mathbf{C}$ is scaled such that it has unit norm. The transmit power distribution for this case is similar to the one shown in Fig. 2 and, therefore, is not shown here. ESPRIT-based DOA estimation is performed for all aforementioned methods. For the traditional MIMO radar-based method, the $MN \times 1$ virtual array is partitioned into two overlapped subarrays of size $(M-1)N \times 1$ each, i.e., the first subarray contains the first $(M-1)N$ elements while the second subarray contains the last $(M-1)N$ elements. For all other methods, the $2N \times 1$ virtual array is partitioned into two non-overlapped subarrays, i.e., the first subarray contains the first N elements while the second subarray contains the last N elements.

The probability of source resolution and the DOA estimation RMSEs versus SNR are shown

for all methods tested in Figs. 8 and 9, respectively. It can be seen from Fig. 8 that the ESPRIT-based DOA estimator for the TS-based MIMO radar with $\zeta = \lambda/2$ has the highest/poorest SNR threshold while the ESPRIT-based DOA estimator for the traditional MIMO radar has the second highest SNR threshold. The ESPRIT-based DOA estimator for the TAP-based MIMO radar has SNR threshold that is lower than the previous two estimators. Moreover, the SNR threshold of the ESPRIT-based DOA estimator for the TS-based MIMO radar with $\zeta = N\lambda/2$ is lower than the SNR threshold of the ESPRIT-based DOA estimator for the TAP-based MIMO radar. Finally, the ESPRIT-based DOA estimator for the proposed transmit beamspace-based MIMO radar has the lowest SNR threshold, i.e., the best probability of source resolution performance.

It can be seen from Fig. 9 that the ESPRIT-based DOA estimator for the TS-based MIMO radar with $\zeta = \lambda/2$ has the highest/poorest RMSE performance. Also this figure shows that the ESPRIT-based DOA estimator for the TAP-based MIMO radar outperforms the ESPRIT-based DOA estimator for the traditional MIMO radar at low SNR region while the opposite occurs at high SNR region. This confirms again the observation from the previous example that having large effective aperture is more important at high SNR region while having high SNR gain per virtual antenna is more important at low SNR region. It can also be observed from Fig. 9 that the ESPRIT-based DOA estimator for the TS-based MIMO radar with $\zeta = N\lambda/2$ outperforms the ESPRIT-based DOA estimator for both the traditional MIMO radar and the TAP-based MIMO radar. Finally, the ESPRIT-based DOA estimator for the proposed transmit beamspace-based MIMO radar outperforms all aforementioned estimators.

VIII. CONCLUSION

A transmit beamspace energy focusing technique for MIMO radar with application to direction finding for multiple targets is proposed. Two methods for focusing the energy of multiple (two or more) transmitted orthogonal waveforms within a certain spatial sector are developed. The essence of the first method is to employ spheroidal sequences for designing transmit beamspace weight matrix so that the SNR gain at each receive antenna is maximized. The subspace decomposition-based techniques such as MUSIC can then be used for direction finding for multiple targets. The second method uses convex optimization to control the amount of dissipated energy in the out-of-sector at the transmitter and to achieve/maintain rotational invariance property at the receiver. This enables the application of search-free DOA estimation techniques such as ESPRIT. Performance analysis of the proposed transmit beamspace-based MIMO radar

and comparison to existing MIMO radar techniques with colocated antennas are given. Stochastic and deterministic CRB expressions as functions of the transmit beamspace weight matrix are found. It is shown that the proposed technique has the lowest CRB as compared to all other techniques. The computational complexity of the proposed method can be controlled by selecting the transmit beamspace dimension, i.e., by selecting the number of transmit beams. Simulation examples show the superiority of the proposed technique over the existing techniques.

REFERENCES

[1] J. Li and P. Stoica, *MIMO Radar Signal Processing*.   New Jersy: Wiley, 2009.

[2] A. Haimovich, R. Blum, and L. Cimini, "MIMO radar with widely separated antennas," *IEEE Signal Processing Magaz.*, vol. 25, pp. 116–129, Jan. 2008.

[3] J. Li and P. Stoica, "MIMO radar with colocated antennas," *IEEE Signal Processing Magaz.*, vol. 24, pp. 106–114, Sept. 2007.

[4] V. F. Pisarenko, "The retrieval of harmonics from a covariance function," *Geophys. J. Royal Astronomical Soc.*, vol. 33, pp. 347-366, 1973.

[5] R. O. Schmidt, "Multiple emitter location and signal parameter estimation," in *Proc. RADC Spectral Estimation Workshop*, Rome, NY, 1979, pp. 234-258.

[6] R. O. Schmidt, "Multiple emitter location and signal parameter estimation," *IEEE Trans. Antennas and Propagation*, vol. 34, pp. 276-280, Mar. 1986.

[7] A. J. Barabell, "Improving the resolution performance of eigenstructure-based direction-finding algorithms," in *Proc. IEEE Int. Conf. on Acoustics, Speech and Signal Processing*, Boston, MA, Apr. 1983, pp. 336-339.

[8] Y. Bresler and A. Macovski, "Exact maximum likelihood parameter estimation of superimposed exponential signals in noise," *IEEE Trans. Acoustics, Speech, and Signal Processing*, vol. 34, no. 10, pp. 1081-1089, Oct. 1986.

[9] R. Roy and T. Kailath, "ESPRIT - estimation of signal parameters via rotational invariance techniques," *IEEE Trans. Acoustics, Speech, and Signal Processing*, vol. 37, no. 7, pp. 984-995, July 1989.

[10] F. Li and R. J. Vaccaro, "Analysis of min-norm and MUSIC with arbitrary array geometry," *IEEE Trans. Aerospace and Electronic Systems*, vol. 26, no. 6, pp. 976-985, Nov. 1990.

[11] M. Viberg and B. Ottersten, "Sensor array processing based on subspace fitting," *IEEE Trans. Signal Processing*, vol. 39, no. 5, pp. 1110-1121, May 1991.

[12] M. Haardt, *Efficient One-, Two-, and Multidimentional High-Resolution Array Signal Processing*, Ph.D. Thesis, Shaker Verlag, Aachen, 1997.

[13] N. D. Sidiropoulos, R. Bro, and G. B. Giannakis, "Parallel factor analysis in sensor array processing," *IEEE Trans. Signal Processing*, vol. 48, no. 8, pp. 2377-2388, Aug. 2000.

[14] S. A. Vorobyov, Y. Rong, N. D. Sidiropoulos, and A. B. Gershman, "Robust iterative fitting of multilinear models," *IEEE Trans. Signal Processing*, vol. 53, no. 8, pp. 2678-2689, Aug. 2005.

[15] L. Xu, J. Li, and P. Stoica, "Target detection and parameter estimation for MIMO radar systems," *IEEE Trans. Aerosp. Electron. Syst.*, vol. 44, no. 3, pp. 927–939, July 2008.

[16] I. Bekkerman and J. Tabrikian, "Target detection and localization using MIMO radars and sonars," *IEEE Trans. Signal Processing*, vol. 54, no. 10, pp. 3873–3883, Oct. 2006.

[17] C. Duofang, C. Baixiao, and Q. Guodong, "Angle estimation using ESPRIT in MIMO radar," *Electronics Letters*, vol. 44, no. 12, pp. 770–771, June 2008.

[18] C. Jinli, G. Hong, and S. Weimin, "Angle estimation using ESPRIT without pairing in MIMO radar," *Electronics Letters*, vol. 44, no. 24, pp. 1422–1423, Nov. 2008.

[19] D. Nion and N. D. Sidiropoulos, "A PARAFAC-based technique for detection and localization of multiple targets in a MIMO radar system," in *Proc. IEEE Int. Conf. Acoustics, Speech and Signal Processing*, Taipei, Taiwan, Apr. 2009, pp. 2077–2080.

[20] P. Stoica and A. Nehorai, "MUSIC, maximum likelihood, and Cramer-Rao bound: further results and comparisons," *IEEE Trans. Acoustics, Speech, and Signal Processing*, vol. 38, no. 12, pp. 2140-2150, Dec. 1990.

[21] H. L. Van Trees, *Optimum Array Processing*, Wiley, NY, 2002.

[22] A. Hassanien and S. A. Vorobyov, "Transmit/receive beamforming for MIMO radar with colocated antennas," in *Proc. IEEE Inter. Conf. Acoustics, Speech, and Signal Processing*, Taipei, Taiwan, Apr. 2009, pp. 2089-2092.

[23] A. Hassanien and S. A. Vorobyov, "Phased-MIMO radar: A tradeoff between phased-array and MIMO radars," *IEEE Trans. Signal Processing*, vol. 58, no. 6, pp. 3137-3151, June 2010.

[24] A. Hassanien and S. A. Vorobyov, "Direction finding for MIMO radar with colocated antennas using transmit beamspace preprocessing," in *Proc. IEEE Inter. Workshop Computational Advances in Multi-Sensor Adaptive Processing*, Aruba, Dutch Antilles, Dec. 2009, pp. 181-184.

[25] A. Hassanien, S. Abd Elkader, A. B. Gershman, and K. M. Wong, "Convex optimization based beamspace preprocessing with an improved robustness against out-of-sector sources," *IEEE Trans. Signal Processing*, vol. 54, pp. 1587-1595, May 2006.

[26] H. B. Lee and M. S. Wengrovitz, "Resolution threshold of beamspace MUSIC for two closely spaced emitters," *IEEE Trans. Acoust., Speech, Signal Processing*, vol. 38, pp. 1545-1559, Sept. 1990.

[27] S. Anderson, "On optimal dimension reduction for sensor array signal processing," *Signal Processing*, vol. 30, pp. 245-256, Jan. 1993.

[28] P. Forster and G. Vezzosi, "Application of spheroidal sequences to array processing," in *Proc. IEEE Inter. Conf. Acoustics, Speech, and Signal Processing*, Dallas, TX, May 1987, pp. 2268-2271.

[29] B. A. Shenoi, *Introduction to Digital Signal Processing and Filter Design*, Wiley & Sons, Hoboken, New Jersey, 2006.

[30] D. J. Rabideau and P. Parker, "Ubiquitous MIMO multifunction digital array radar," in *Proc. 37th Asilomar Conf. on Signals, Systems, and Computer*, Nov. 2003, vol. 1, pp. 1057–1064.

[31] J. Bergin, S. McNeil, L. Fomundam, and P. Zulch, "MIMO phased-array for SMTI radar," in *Proc. IEEE Aerospace Conf.*, Big Sky, MT, Mar. 2008, pp. 1–7.

[32] P. Stoica, E. G. Larsson, and A. B. Gershman, "The stochastic CRB for array processing: A textbook derivation," *IEEE Signal Processing Letters*, vol. 8, pp. 148-150, May 2001.

[33] P. Stoica and A. Nehorai, "Performance study of conditional and unconditional direction-of-arrival estimation," *IEEE Trans. Acoust., Speech, Signal Processing*, vol. 38, pp. 1783–1795 , Oct. 1990.
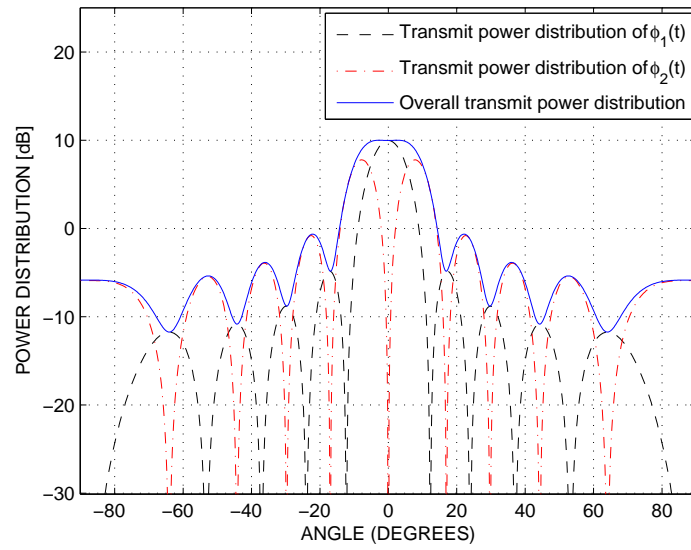
Fig. 1. Transmit beamspace beampattern using spheroidal sequences without rotation. Total transmit power is uniformly distributed within the desired spatial sector, however, different transmitted waveforms have different power distribution.
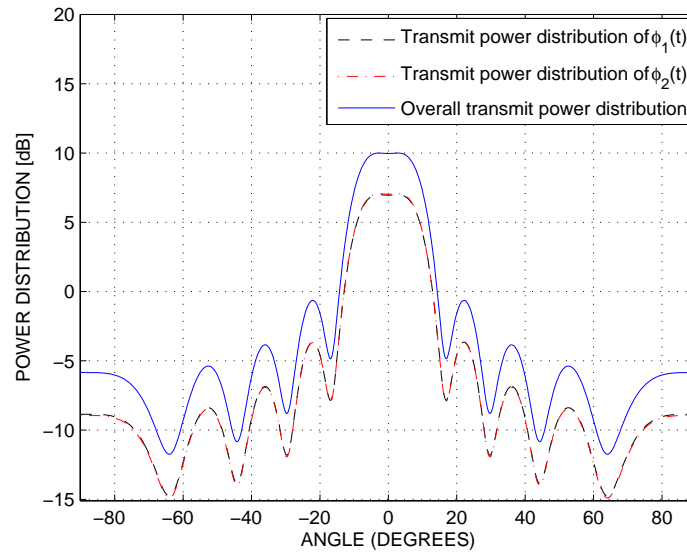
Fig. 2.   Transmit beamspace beampattern using spheroidal sequences with rotation. Total transmit power as well as individual waveform powers are uniformly distributed within the desired spatial sector.
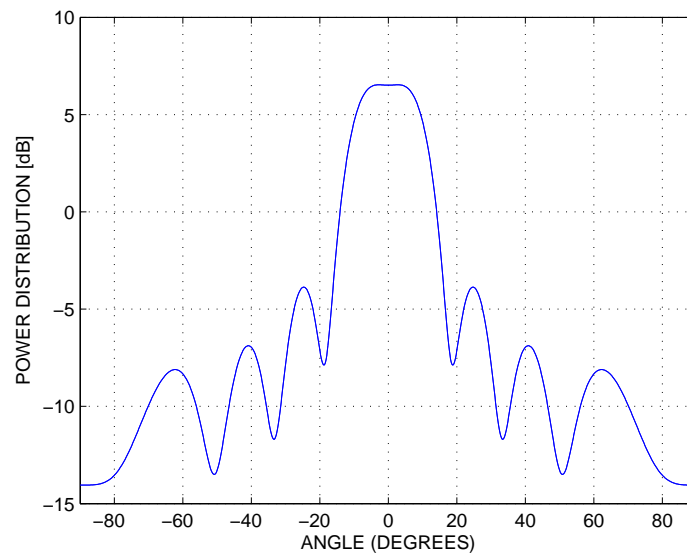

Fig. 3.   TAP-based MIMO radar transmit beampattern using two fully overlapped subarrays.
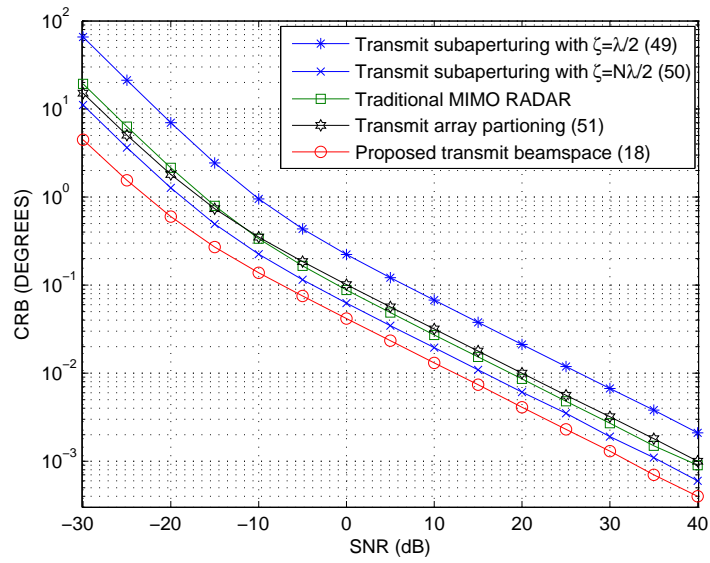
Fig. 4. Stochastic CRB versus SNR.
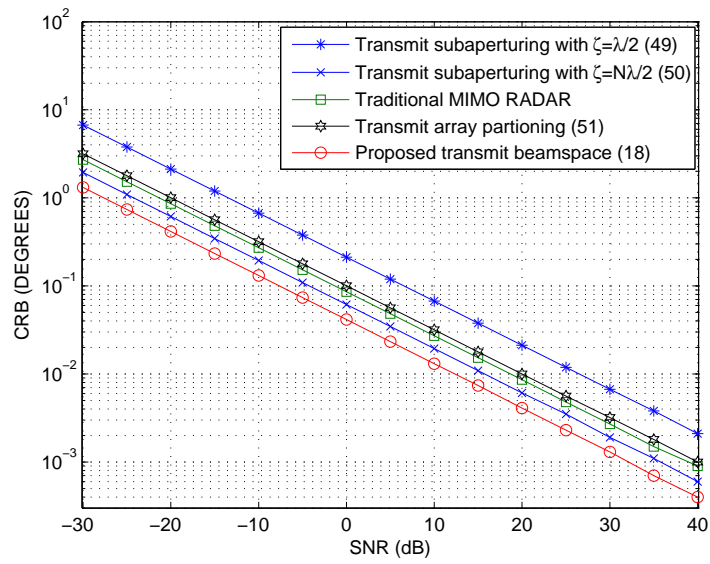
Fig. 5. Deterministic CRB versus SNR.
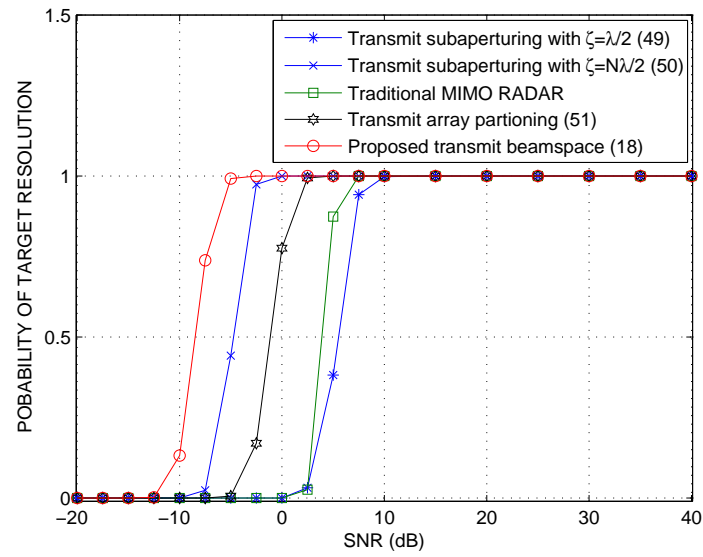
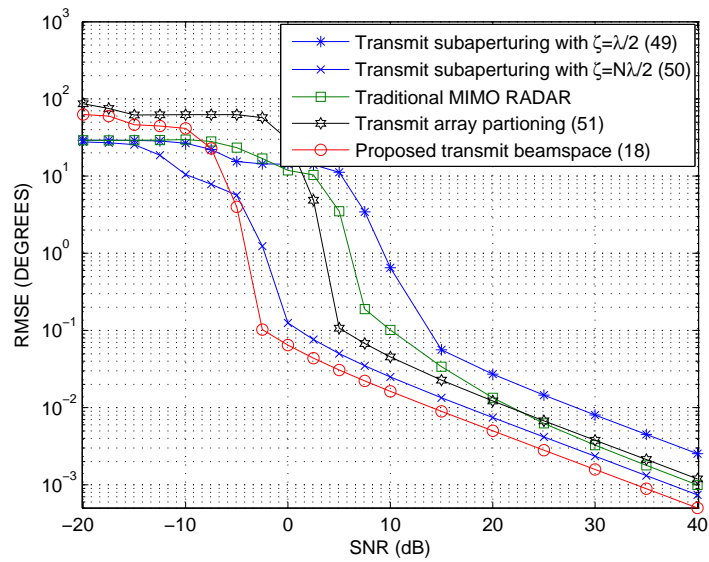Fig. 6. Probability of target resolution versus SNR for MUSIC-based DOA estimators.

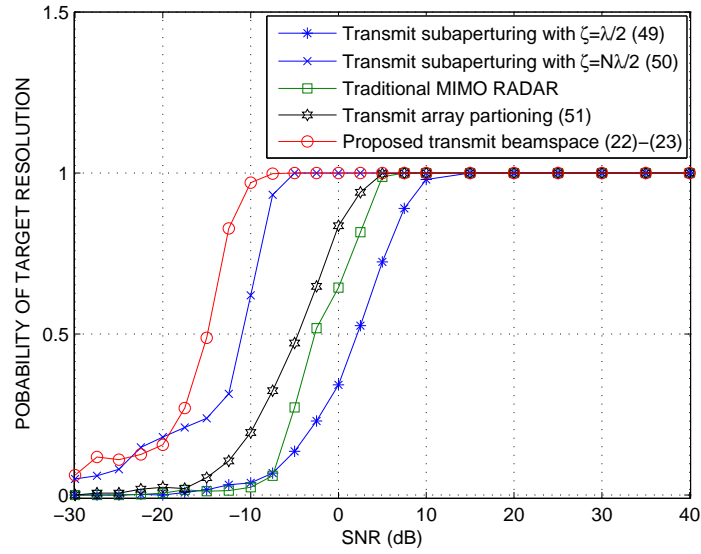Fig. 7. RMSE versus SNR for MUSIC-based DOA estimators.

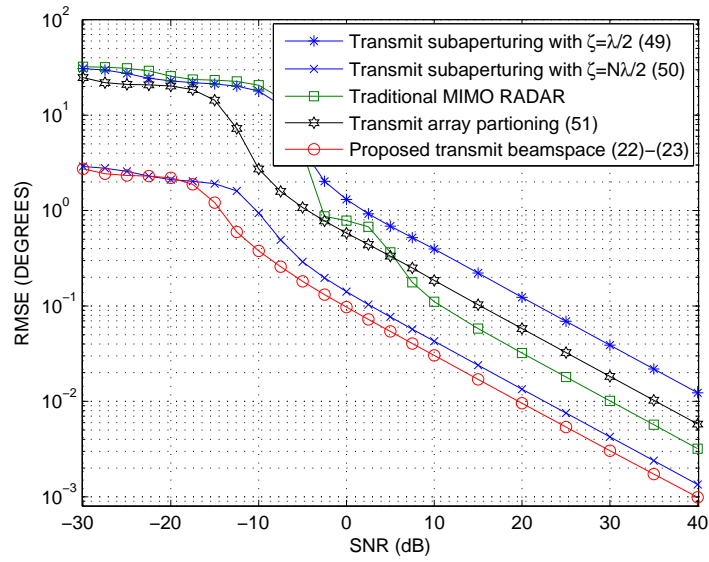Fig. 8. Probability of target resolution versus SNR for ESPRIT-based DOA estimators.

Fig. 9. RMSE versus SNR for ESPRIT-based DOA estimators.